Supplementary Information for

Dichlorido-bridged dinuclear Dy(III) single-molecule magnet with an effective energy barrier larger than 600 K

Tian Han,‡[a] You-Song Ding,‡[a,b] Zi-Han Li,[a] Ke-Xin Yu,[a] Yuan-Qi Zhai,[a] Nicholas F. Chilton*[b] and Yan-Zhen Zheng*[a]

[a] School of Science, and Frontier Institute of Science and Technology (FIST), State Key Laboratory for Mechanical Behavior of Materials, MOE Key Laboratory for Nonequilibrium Synthesis and Modulation of Condensed Matter, Xi'an Key Laboratory of Sustainable Energy and Materials Chemistry, Xi'an Jiaotong University, Xi'an 710049, China. E-mail: zheng.yanzhen@xjtu.edu.cn

[b] School of Chemistry, The University of Manchester, Oxford Road, Manchester M13 9PL, United Kingdom

Corresponding email: zheng.yanzhen@xjtu.edu.cn; nicholas.chilton@manchester.ac.uk

1 Experimental

1.1 Materials and method

All reactions were carried out under a dry and oxygen-free argon atmosphere by using Schlenk techniques or in a glovebox. All solvents were dried and degassed by standard techniques. Anhydrous $LnCl_3$ salts were prepared according to the literature procedure.[1] The ligands were commercially available and used without further treatment. NMR spectra were measured on a Bruker Avance-400 spectrometer and chemical shifts (δ) are reported in parts per million (ppm). ^{1}H NMR spectra were recorded at 400 MHz in NMR solvents and referenced internally to corresponding solvent resonance. Elemental analyses were performed on a Flash 2000 elemental analyser. Infrared spectra were collected on a Thermo Fisher Nicolet 6700 FT-IR spectrometer using ATR (Attenuated Total Reflectance) method. Absorption maxima (ν max) are reported in wavenumbers (cm^{-1}).

1.2 Syntheses of complexes 1–4

Synthesis of complex 1. In an argon glovebox, 8 ml THF was added to a Schlenk tube containing $LiN(Cy)_2$ (0.275 g, 1.5 mmol, prepared by deprotonation $HN(Cy)_2$ with Li-^{n}Bu), $DyCl_3$ (0.268 g, 0.1 mmol) and a stir bar. After stirring for 12 h, the solvent was removed by vacuum. And the crystalline product was extract with pentane (3×5 ml) which was concentrated to 5 ml. The product was obtained as yellow crystals after standing for 1 d. Yield 122 mg, 19 %. Elemental analysis calcd (%) for $C_{56}H_{104}Cl_2Dy_2N_4O_2$: C 53.32, H 8.31, N 4.44; found: C 53.73, H 8.72 N 4.10. IR (KBr, cm^{-1}): 2662 (m), 1447 (m), 1400 (h), 1345 (w), 1312 (w), 1246 (m), 1158 (w), 1144 (s), 1122 (s), 1046 (m), 984 (m), 950 (m), 918 (w), 861 (m, br), 842 (m), 799 (m), 777 (m), 663 (m).

Synthesis of complex 2. The synthesis is the same as **1** with anhydrous $DyCl_3$ replaced by 0.5 mmol of anhydrous $GdCl_3$. Yield 156 mg, 24.9 %. Elemental analysis calcd (%) for $C_{56}H_{104}Cl_2Gd_2N_4O_2$: C 53.77, H 8.38, N 4.48; found: C 53.51, H 8.73 N 4.25. IR (KBr, cm^{-1}): 2661(m), 1448 (m), 1402 (h), 1345 (w), 1327 (w), 1249 (m), 1158 (w), 1145 (s), 1122 (s), 1035 (m), 984 (m, br), 948 (m), 917 (w), 888 (m, br), 842 (m), 798 (m), 776 (m), 665 (s).

Synthesis of complex 3. The synthesis is the same as **1** with anhydrous $DyCl_3$ replaced by 0.5 mmol of anhydrous YCl_3. Yield 86 mg, 15.4 %. Elemental analysis calcd (%) for $C_{56}H_{104}Cl_2Y_2N_4O_2$: C 60.37, H 9.41, N 5.03; found: C 60.60 H 9.81 N 4.50. ^{1}H-NMR (C_6D_6, 400 MHz): 3.57 (m, 8H), 3.34 (s,4H), 3.13 (s, 4H), 1.43-0.85 (m, 88H). IR (KBr, cm^{-1}): 2626 (m), 1456 (s), 1399 (s), 1338 (w), 1313 (w), 1255 (m), 1139 (m, br), 1056 (m), 965 (w), 949 (w), 919 (w), 895 (w), 850 (m).

Synthesis of complex 4 (6 %). The synthesis is the same as **1** with anhydrous $DyCl_3$ replaced by 0.475 mmol of anhydrous YCl_3 and 0.025 mmol of anhydrous $DyCl_3$. Elemental analysis calcd (%)

for $C_{56}H_{104}Cl_2Y_{1.88}Dy_{0.12}N_4O_2$: C 59.89, H 9.33, N 4.99; found: C 60.11 H 9.49 N 4.70. The resultant mole ratio of Y:Dy in **4** is determined by its magnetic susceptibility at room temperature and magnetization at 7 T and 2 K.

2. X-ray Crystallography Data

All data were recorded on a Bruker SMART CCD diffractometer with MoKα radiation (λ = 0.71073 Å). The structures were solved by direct methods and refined on F^2 using SHELXTL. CCDC 1420401 (**1**), 1560851 (**2**) and 1560852 (**3**) contain the supplementary crystallographic data for this paper. These data can be obtained free of charge via www.ccdc.cam.ac.uk/conts/retrieving.html (or from the Cambridge Crystallographic Data Centre, 12 Union Road, Cambridge CB21EZ, UK; fax: (+44)1223-336-033; or deposit@ccdc.cam.ac.uk).

Table S1 Crystallographic data for complexes **1**–**3**.

Compound	**1**	**2**	**3**
Formula	$C_{56}H_{104}Cl_2Dy_2N_4O_2$	$C_{56}H_{104}Cl_2Gd_2N_4O_2$	$C_{56}H_{104}Cl_2Y_2N_4O_2$
M, g mol^{-1}	1261.33	1250.83	1114.15
Temperature, K	100(2)	100(2)	100(2)
Space group	P-1	P-1	P-1
a, Å	11.0806(8)	11.095(2)	11.0839(17)
b, Å	11.5773(9)	11.523(2)	11.5625(18)
c, Å	13.7888(10)	13.869(3)	13.800(2)
α, deg	108.8510(10)	108.507(2)	108.736(2)
β, deg	105.6940(10)	106.262(2)	105.790(2)
γ, deg	102.0520(10)	101.839(2)	102.087(2)
V, Å^3	1524.0(2)	1527.6(5)	1523.8(4)
Z	1	1	1
d_{cal}, g cm^{-3}	1.374	1.360	1.214
2θ range, deg	3.352 to 55.13	3.336 to 49.168	3.35 to 49.854
Completeness	0.981	0.976	0.983
Final indices [$I>2\sigma(I)$]	R_1 = 0.0236, wR_2 = 0.0531	R_1 = 0.0224, wR_2 = 0.0516	R_1 = 0.0366, wR_2 = 0.0793
R indices (all data)	R_1 = 0.0275, wR_2 = 0.0549	R_1 = 0.0268, wR_2 = 0.0531	R_1 = 0.0540, wR_2 = 0.0842
Goodness-of-fit on F^2	1.075	1.066	1.041
Residual map, e Å^{-3}	1.02/-0.47	0.80/-0.40	0.54/-0.26

Table S2 Selected bond lengths (Å) and angles (deg) for complex **1**.

Dy(1)-N(1)	2.169(2)	Dy(1)-N(2)	2.174(2)
Dy(1)-O(1)	2.436(2)	Dy(1)-Cl(1)#1	2.7198(7)
Dy(1)-Cl(1)	2.7469(7)	N(1)-Dy(1)-N(2)	118.17(9)
N(1)-Dy(1)-O(1)	90.44(8)	N(2)-Dy(1)-O(1)	97.23(8)
N(1)-Dy(1)-Cl(1)#1	127.49(6)	N(2)-Dy(1)-Cl(1)#1	114.28(6)
O(1)-Dy(1)-Cl(1)#1	80.72(5)	N(1)-Dy(1)-Cl(1)	95.99(6)
N(2)-Dy(1)-Cl(1)	99.58(6)	O(1)-Dy(1)-Cl(1)	156.45(6)
Cl(1)#1-Dy(1)-Cl(1)	77.39(2)	Dy(1)#1-Cl(1)-Dy(1)	102.61(2)

[a]Symmetry codes: #1 -x+2, -y+1, -z

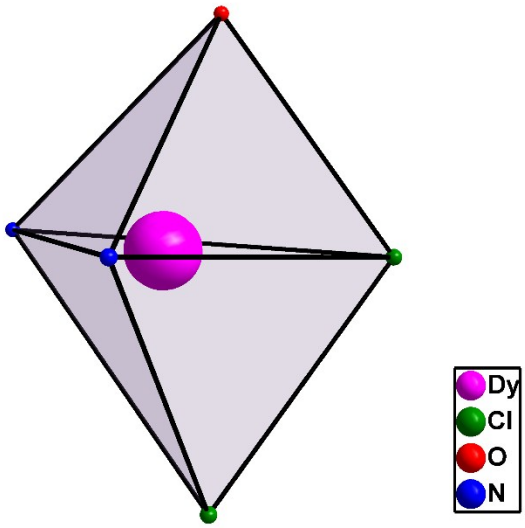

Fig. S1 Local coordination environment of dysprosium ion in complex **1**.

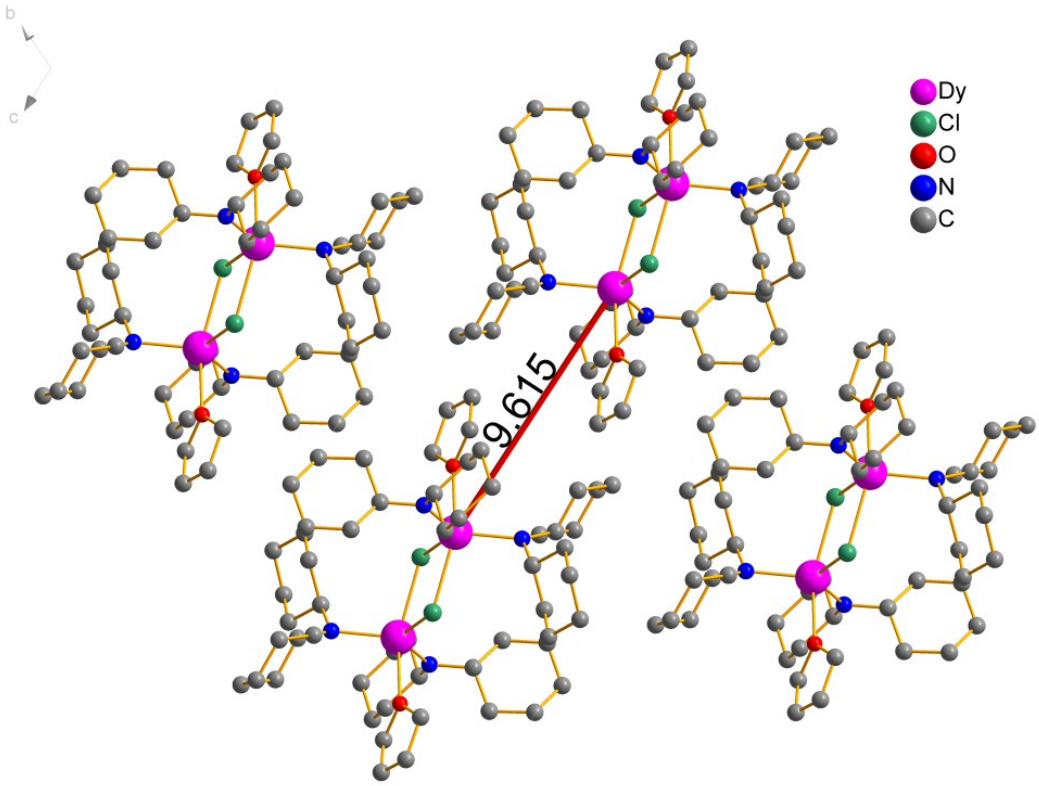

Fig. S2 Packing diagram for complex **1**.

3. Magnetic Properties

Magnetic susceptibility measurements have been carried out with a Quantum Design MPMS-XL7 SQUID magnetometer upon cooling from 300 to 2 K in variable applied fields. Ac susceptibility measurements have been performed at frequencies of between 1 and 1500 Hz with an oscillating field of 3.5 Oe and with variable dc applied field. Powder samples were embedded in eicosane to avoid any field induced crystal reorientation. A diamagnetic correction has been calculated from Pascal constants and embedding eicosane has been applied to the observed magnetic susceptibility.

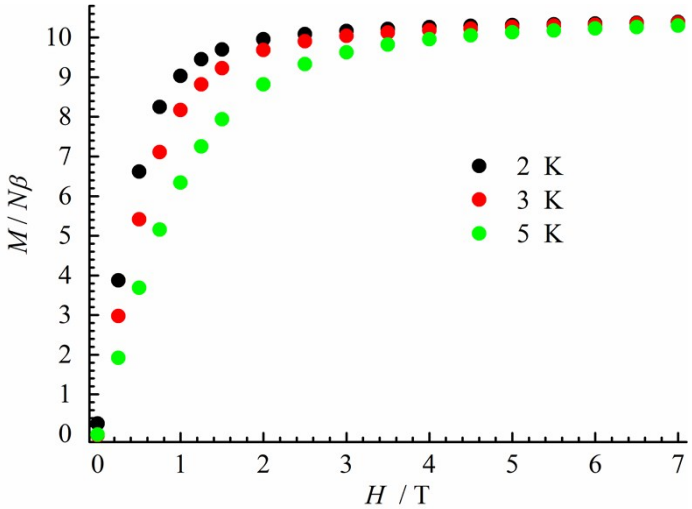

Fig. S3 The field dependence of the magnetization for **1**.

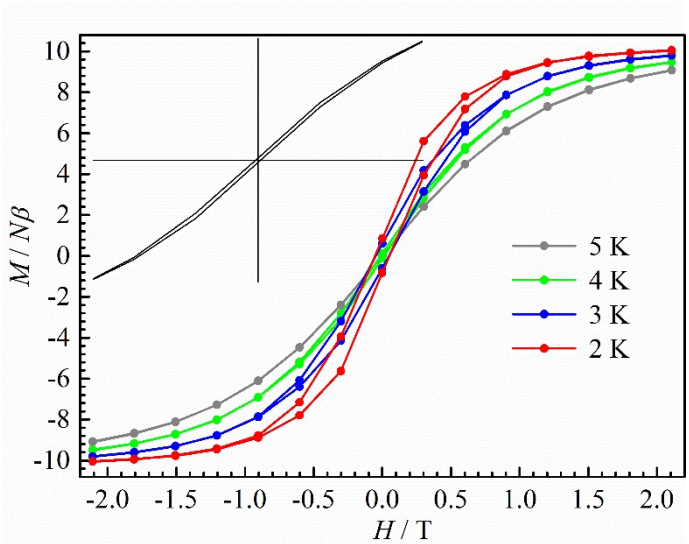

Fig. S4 Magnetic hysteresis measurements for **1** with an average sweep rate of 2.5 mT s^{-1} at indicated temperature. Inset: Magnetic hysteresis for **1** at 4 K.

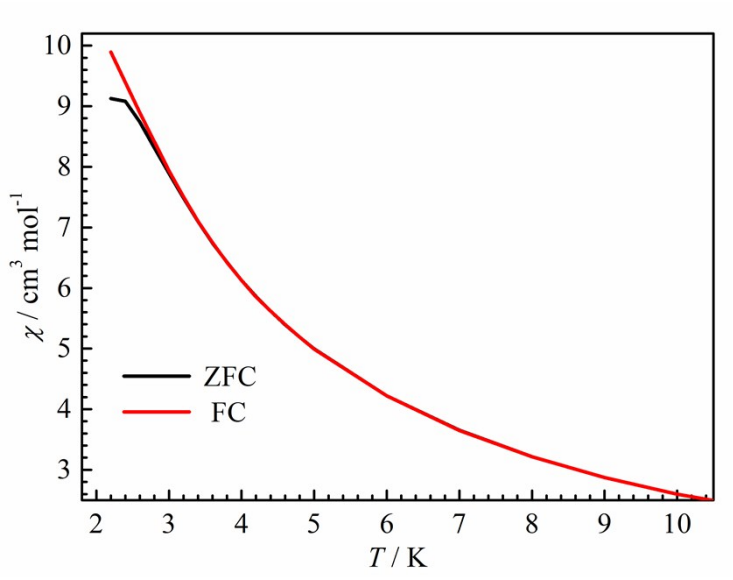

Fig. S5 FC and ZFC of **1** at an applied field of 0.2 T.

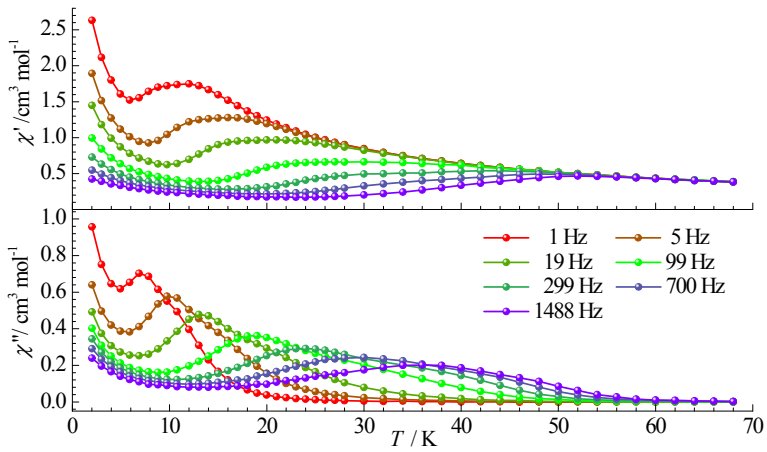

Fig. S6 Temperature-dependence of the χ' and χ'' ac susceptibility signals under zero dc field at the indicated frequencies for **1**. Solid lines are guide for vision.

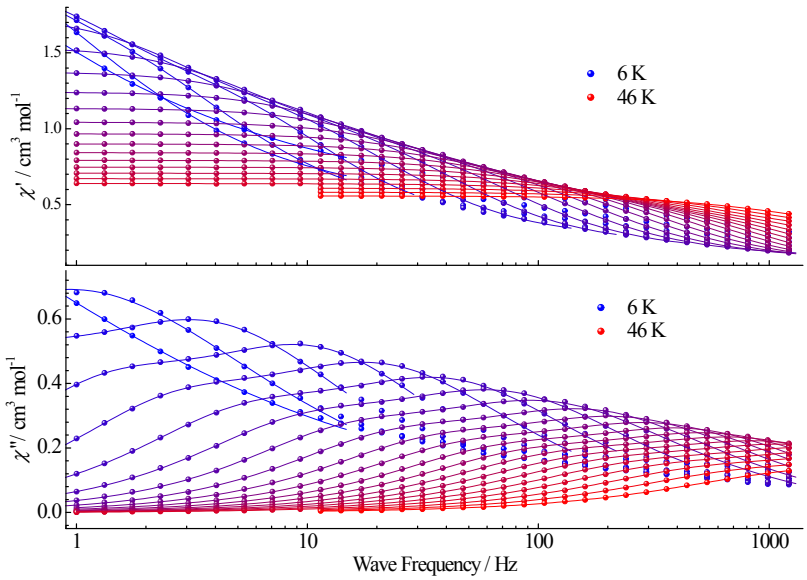

Fig. S7 Frequency-dependence of the in-phase (χ', top) and out-of-phase (χ'', bottom) ac susceptibility signals under zero dc field at the temperature from 6.0 K (blue) to 46 K (red) for **1**. The solid lines are the best fit.

Table S3 Relaxation Fitting Parameters for **1**.

T	τ	α	χ_S	χ_T			
6[a]	5.56139	0.57295	7.09085	0.45688			
8	0.16944	0.32408	2.84602	0.49015			
	$\chi_{s,tol}$	χ_1	τ_1	α_1	χ_2	τ_2	α_2
10	0.43624	2.84594	0.03984	0.17647	1.26756	0.43314	0
12	0.35688	2.68374	0.01403	0.10841	0.98779	0.12914	0.02118
14	0.2662	2.02768	0.00711	0.13755	0.93386	0.06489	2.50E-03
16	0.22669	1.60655	0.00361	0.11198	0.98146	0.03222	2.58E-02
18	0.18924	1.43681	0.00207	0.10939	0.89894	0.01809	3.13E-02
20	0.15321	1.53656	0.00134	0.13235	0.66396	0.01167	6.97E-03
22	0.14072	1.32266	8.62E-04	0.10685	0.67071	0.00741	1.99E-02
24	0.1213	0.93938	6.05E-04	0.11529	0.89022	0.0051	0.02229
26	0.11269	0.80972	4.31E-04	0.09982	0.9514	0.0036	0.03162
28	0.11073	0.70928	3.15E-04	0.07201	0.96835	0.00256	0.04273
30	0.09672	0.75286	2.41E-04	0.0815	0.73436	0.00194	0.0431
32	0.08897	0.6337	1.83E-04	0.07162	0.84996	0.00143	0.0535
34	0.07897	0.68278	1.42E-04	0.07733	0.64595	0.0011	0.05739
36	0.07061	0.69481	1.08E-04	0.07621	0.56208	8.38E-04	0.06536
38	0.09117	0.75974	8.52E-05	0.01024	0.44814	6.05E-04	0.07574
40	0.01865	0.61732	5.09E-05	0.11544	0.62569	4.63E-04	0.07288
42	0[b]	0.71215	3.16E-05	0.03916	0.4987	3.09E-04	0.09282
44	0	0.71179	2.12E-05	0	0.46076	2.08E-04	0.10702
46	0	0.56057	1.40E-05	0	0.55377	1.31E-04	0.12327

[a] Those parts was fitting with one generalized Debye function for only the FR could be observed at those temperature. [b]These parameter values were fixed to 0.

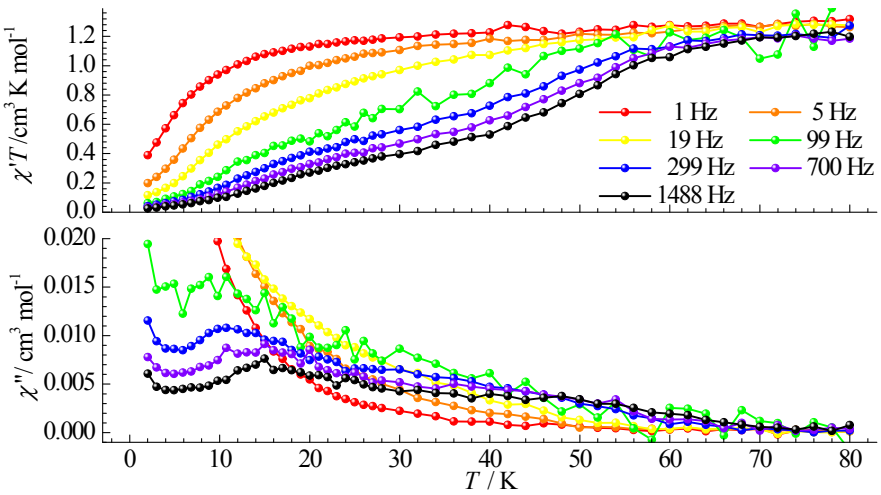

Fig. S8 Temperature-dependence of the in-phase (χ') and out-of-phase (χ'') ac susceptibility signals under zero dc field at the indicated frequencies for **4**.

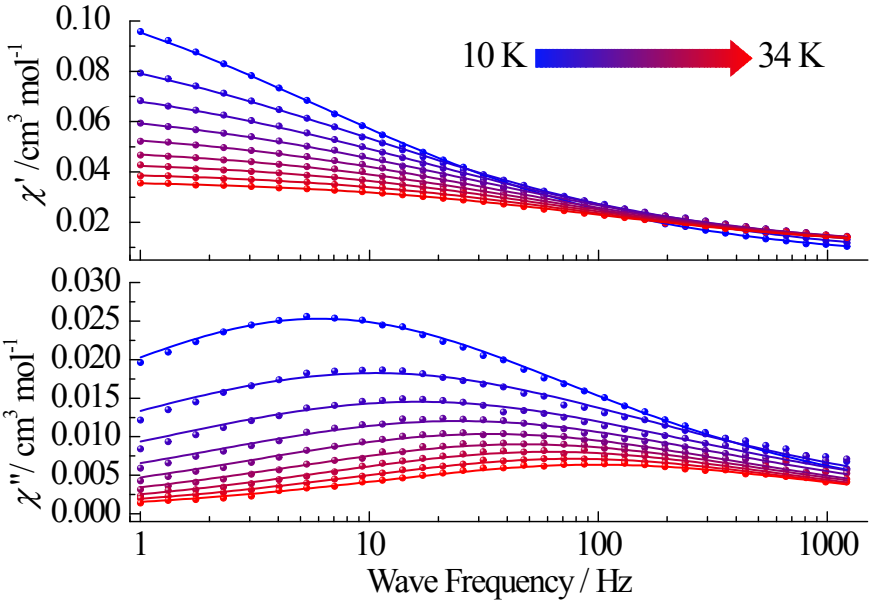

Fig. S9 Frequency-dependence of the in-phase (χ', top) and out-of-phase (χ'', bottom) ac susceptibility signals under zero dc field at the temperature from 10.0 K (blue) to 34 K (red) for **4**. The solid lines are the best fit.

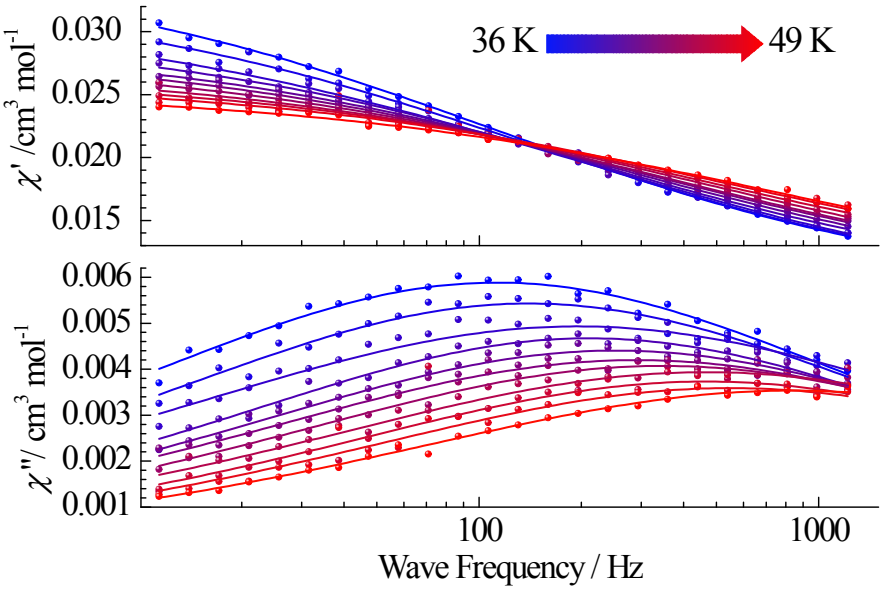

Fig. S10 Frequency-dependence of the in-phase (χ', top) and out-of-phase (χ'', bottom) ac susceptibility signals under zero dc field at the temperature from 36 K (blue) to 49 K (red) for **4**. The solid lines are the best fit.

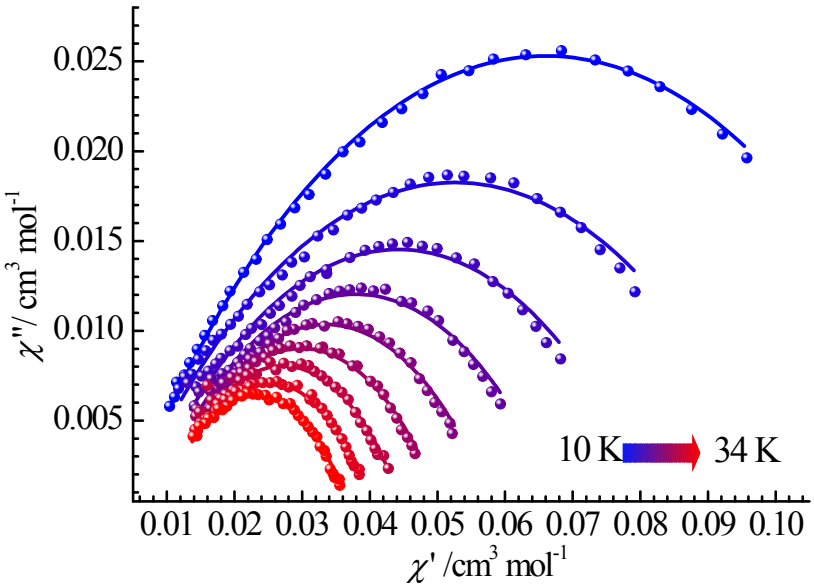

Fig. S11 Cole-Cole plots using the frequency-dependence ac susceptibility data under zero dc field for **4** from 10.0 K (blue) to 34 K (red). The solid lines are the best fits.

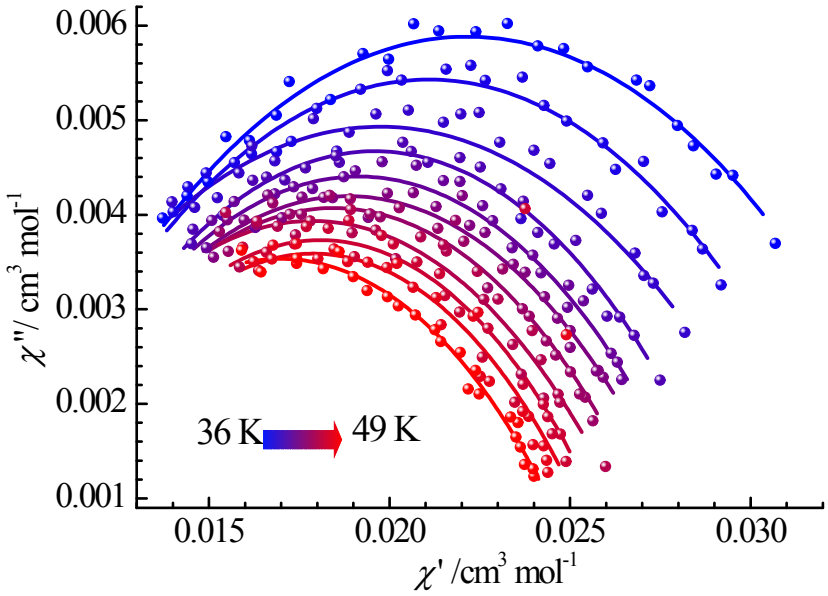

Fig. S12 Cole-Cole plots using the frequency-dependence ac susceptibility data under zero dc field for **4** from 36 K (blue) to 49 K (red). The solid lines are the best fits.

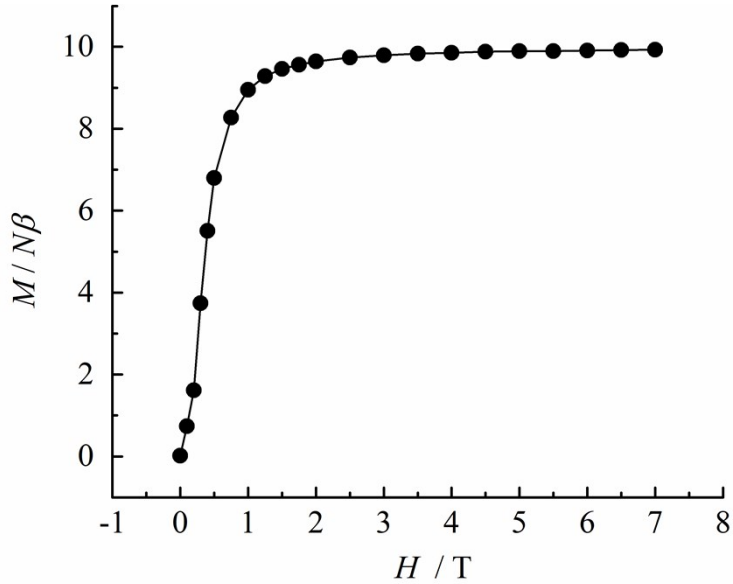

Fig. S13 Field dependence of the magnetization for **4** at 2 K (scaled for two Dy^{III} ions).

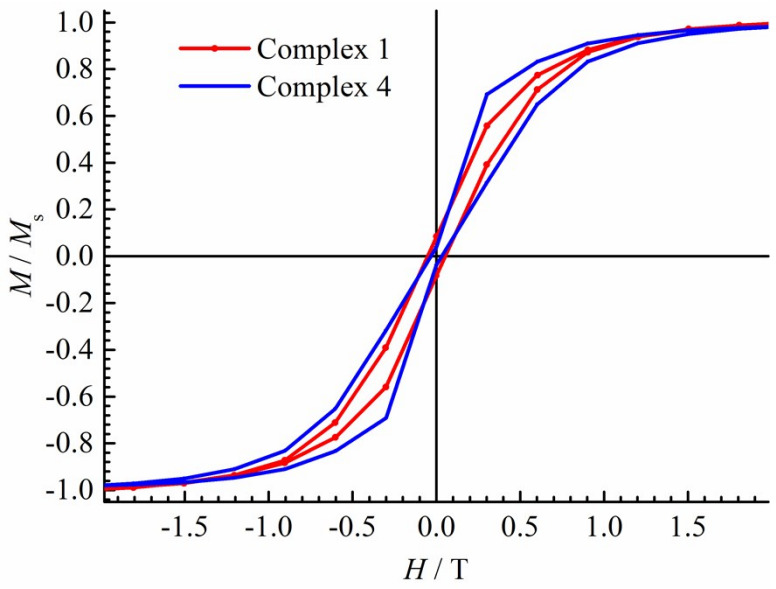

Fig. S14 Magnetic hysteresis for **1** and **4** with an average sweep rate of 2.5 mT s^{-1} at 2 K.

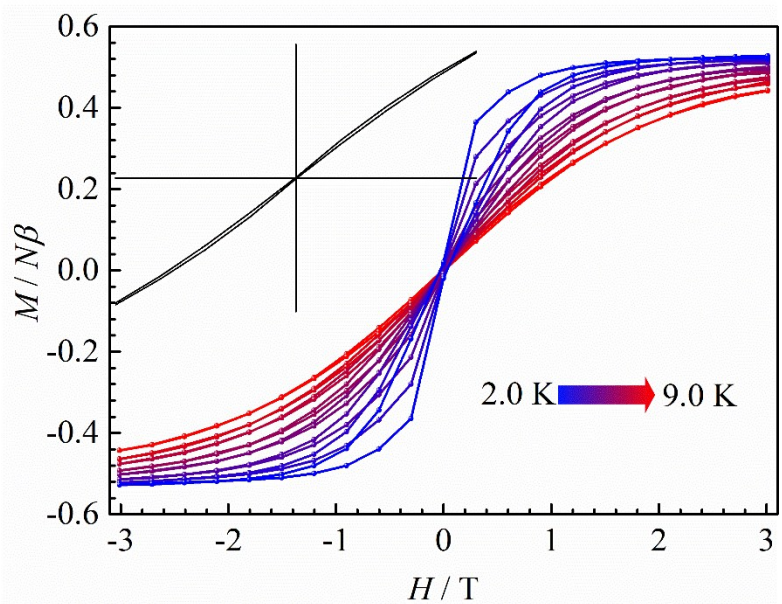

Fig. S15 Magnetic hysteresis measurements for **4** with an average sweep rate of 2.5 mT s^{-1} from 2 K to 9 K. Inset: Magnetic hysteresis for **4** at 9 K.

Table S4 CASSCF-SO results for **1**.

Energy (cm^{-1})	gx	gy	gz	Angle (°)[a]	Crystal Field Wavefunction[b]
0	0.00	0.00	19.78	--	$98\%\left\lvert \pm\frac{15}{2}\right\rangle$
273	0.01	0.01	16.84	4.0	$92\%\left\lvert \pm\frac{13}{2}\right\rangle$
460	0.11	0.13	14.09	10.9	$86\%\left\lvert \pm\frac{11}{2}\right\rangle + 10\%\left\lvert \pm\frac{7}{2}\right\rangle$
588	0.60	0.84	11.54	19.5	$77\%\left\lvert \pm\frac{9}{2}\right\rangle + 10\%\left\lvert \pm\frac{5}{2}\right\rangle$
688	1.85	4.08	8.53	22.9	$37\%\left\lvert \pm\frac{7}{2}\right\rangle + 28\%\left\lvert \mp\frac{7}{2}\right\rangle$
752	3.18	4.25	11.84	84.4	$24\%\left\lvert \pm\frac{5}{2}\right\rangle + 17\%\left\lvert \pm\frac{3}{2}\right\rangle + 17\%\left\lvert \mp\frac{1}{2}\right\rangle + 15\%\left\lvert \mp\frac{5}{2}\right\rangle + 12$
803	0.69	2.22	14.23	85.3	$23\%\left\lvert \pm\frac{3}{2}\right\rangle + 18\%\left\lvert \pm\frac{5}{2}\right\rangle + 16\%\left\lvert \mp\frac{3}{2}\right\rangle + 11\%\left\lvert \mp\frac{5}{2}\right\rangle + 11$
1008	0.01	0.02	19.43	88.1	$33\%\left\lvert \pm\frac{1}{2}\right\rangle + 17\%\left\lvert \mp\frac{3}{2}\right\rangle + 15\%\left\lvert \pm\frac{3}{2}\right\rangle + 14\%\left\lvert \mp\frac{1}{2}\right\rangle$

[a] Angle that largest *g*-tensor component makes with g_z of ground Kramers doublet.
[b] Quantisation axis taken as g_z direction of ground Kramers doublet (Fig. 2), components with > 10% contribution given, rounded to nearest percent.

Table S5 The two shortest coordination bonds and their angles of some high performance single-ion anisotropy dominant Dy(III) SMMs.

Complex	Ln-X (Å)	Ln-X (Å)	Angle (°)	*ΔE* (K)	ref
$[Dy_2(NO_3)_4(sacbH)_2(H_2O)_2(MeCN)_2]$	2.231	2.305	150.72	109	2
$[Dy(OPCy_3)_2(H_2O)_5]Cl_3$	2.217	2.221	175.79	472	3
$[Dy(OPCy_3)_2(H_2O)_5]Br_3$	2.189	2.210	179.04	543	3
$[Dy(Cy_2N)_2(\mu\text{-}Cl)(THF)]_2$	2.169	2.174	118.19	633	This work
Dy(bbpen)Cl	2.166	2.166	154.3	708	4
$[Dy(m\text{-}OH)(DBP)_2(THF)]_2$	2.094	2.120	108.83	721	5
$[Dy(OP^tBu(NH^iPr_2)_2)_2(H_2O)_5]^{3+}$	2.203	2.208	175.14	735	6
$(NN^{TBS})DyI(THF)$	2.206	2.212	134.75	770	7
$[Ln(BIPM^{TMS})_2][K(18C6)(THF)_2]$	2.433	2.434	176.6	810	8
Dy(bbpen)Br	2.163	2.163	155.8	1025	4
$[Dy(O^tBu)_2(py)_5][BPh_4]$	2.110	2.114	178.91	1815	9

$sacbH_2$ = N-salicylidene-2-amino-5-chlorobenzoic acid; bbpen = *N,N'*bis(2-hydroxybenzyl)-*N,N'*-bis(2-methylpyridyl)ethylene-diamine; DBP^- = 2,6-ditert-butylphenolate; NN^{TBS} = 1,1′-ferrocenediyl (NHSitBuMe2)2 , $BIPM^{TMS}$ = $\{C(PPh_2NSiMe_3)_2\}^{2-}$;

References:

1. J. B. Reed, B. Hopkins, L. Audrieth, P. Selwood, R. Ward and J. Dejong, *Inorganic Syntheses, Volume 1*, 28-33.
2. E. C. Mazarakioti, J. Regier, L. Cunha-Silva, W. Wernsdorfer, M. Pilkington, J. Tang and T. C. Stamatatos, *Inorg. Chem.*, 2017, **56**, 3568-3578.
3. Y. C. Chen, J. L. Liu, L. Ungur, J. Liu, Q. W. Li, L. F. Wang, Z. P. Ni, L. F. Chibotaru, X. M. Chen and M. L. Tong, *J. Am. Chem. Soc.*, 2016, **138**, 2829-2837.
4. J. Liu, Y. C. Chen, J. L. Liu, V. Vieru, L. Ungur, J. H. Jia, L. F. Chibotaru, Y. H. Lan, W. Wernsdorfer, S. Gao, X. M. Chen and M. L. Tong, *J. Am. Chem. Soc.*, 2016, **138**, 5441-5450.
5. J. Xiong, H. Y. Ding, Y. S. Meng, C. Gao, X. J. Zhang, Z. S. Meng, Y. Q. Zhang, W. Shi, B. W. Wang and S. Gao, *Chem. Sci.*, 2017, **8**, 1288-1294.
6. S. K. Gupta, T. Rajeshkumar, G. Rajaraman and R. Murugavel, *Chem Sci*, 2016, **7**, 5181-5191.
7. K. L. Harriman, J. L. Brosmer, L. Ungur, P. L. Diaconescu and M. Murugesu, *J. Am. Chem. Soc.. 139*, 1420-1423.
8. M. Gregson, N. F. Chilton, A. M. Ariciu, F. Tuna, I. F. Crowe, W. Lewis, A. J. Blake, D. Collison, E. J. L. McInnes, R. E. P. Winpenny and S. T. Liddle, *Chem. Sci.*, 2016, **7**, 155-165.
9. Y. S. Ding, N. F. Chilton, R. E. P. Winpenny and Y. Z. Zheng, *Angew. Chem. Int. Edit.*, 2016, **55**, 16071-16074.